AD-A039 765 COLORADO STATE UNIV FORT COLLINS DEPT OF CHEMISTRY F/G 20/2
VIBRATIONAL SPECTRA OF TRANSITION METAL HEXAFLUORIDE CRYSTALS. --ETC(U)
APR 77 E R BERNSTEIN, G R MEREDITH N00014-75-C-1179
UNCLASSIFIED TR-12 NL

1 OF 1
ADA039 765

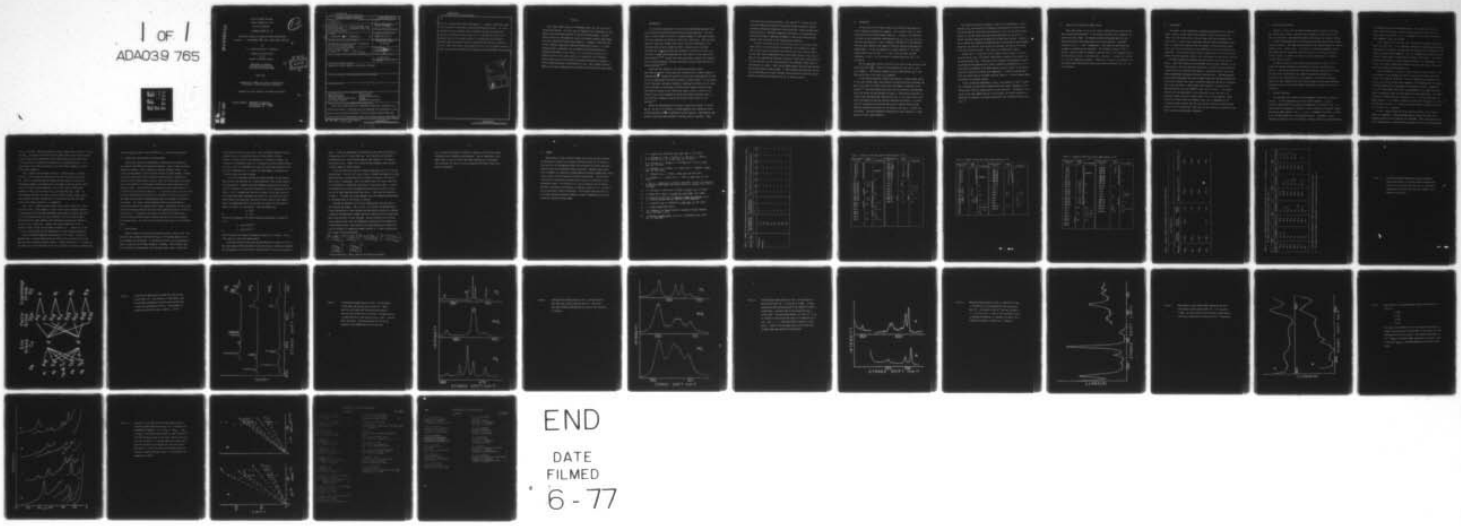

END

DATE
FILMED
6-77

OFFICE OF NAVAL RESEARCH

Contract N00014-75-C-1179

Task No. NR 056-607

TECHNICAL REPORT NO. 12

"Vibrational Spectra of Transition Metal Hexafluoride Crystals. I. Orthorhombic MoF_6, WF_6, and UF_6 Neat Crystals"

by

E. R. Bernstein and G. R. Meredith*

Prepared for Publication
in the
Journal of Chemical Physics

Department of Chemistry
Colorado State University
Fort Collins, Colorado 80523

April 1977

*Current address: Department of Chemistry
University of Pennsylvania
Philadelphia, PA 19174

UNCLASSIFIED

SECURITY CLASSIFICATION OF THIS PAGE *(When Data Entered)*

REPORT DOCUMENTATION PAGE		READ INSTRUCTIONS BEFORE COMPLETING FORM
1. REPORT NUMBER (14) TR-12	2. GOVT ACCESSION NO.	3. RECIPIENT'S CATALOG NUMBER (9)
4. TITLE *(and Subtitle)* (6) "Vibrational Spectra of Transition Metal Hexafluoride Crystals. I. Orthorhombic MoF_6, WF_6, and UF_6 Neat Crystals."		5. TYPE OF REPORT & PERIOD COVERED Technical Report
		6. PERFORMING ORG. REPORT NUMBER
7. AUTHOR(s) (10) E. R. Bernstein [redacted] G. R. Meredith		8. CONTRACT OR GRANT NUMBER(s) (15) N00014-75-C-1179
9. PERFORMING ORGANIZATION NAME AND ADDRESS Colorado State University, Dept. of Chemistry Fort Collins, Colorado 80523		10. PROGRAM ELEMENT, PROJECT, TASK AREA & WORK UNIT NUMBERS NR 056-607
11. CONTROLLING OFFICE NAME AND ADDRESS Office of Naval Research Arlington, VA 22217 (12) 43 P.		12. REPORT DATE (11) April 1977
		13. NUMBER OF PAGES 45
14. MONITORING AGENCY NAME & ADDRESS *(if different from Controlling Office)*		15. SECURITY CLASS. *(of this report)* Unclassified
		15a. DECLASSIFICATION/ DOWNGRADING SCHEDULE

16. DISTRIBUTION STATEMENT *(of this Report)*

Approved for Public Release; Distribution Unlimited.

17. DISTRIBUTION STATEMENT *(of the abstract entered in Block 20, if different from Report)*

2- A039 857

3- A039 793

18. SUPPLEMENTARY NOTES

19. KEY WORDS *(Continue on reverse side if necessary and identify by block number)*

Raman scattering
molecular crystals
transition metal hexafluorides
pure crystal spectra
mixed crystals
exciton band structure
phonons
two-particle transitions

20. ABSTRACT *(Continue on reverse side if necessary and identify by block number)*

Neat crystal Raman spectra of orthorhombic MoF_6, WF_6, and UF_6 are presented and discussed. This work lays the foundation for presentation of two-particle and total band structures in the two following papers. The neat crystal spectra are interpreted in terms of an internal-external mode separa-

DD FORM 1 JAN 73 1473 EDITION OF 1 NOV 65 IS OBSOLETE S/N 0102-014-6601

UNCLASSIFIED

SECURITY CLASSIFICATION OF THIS PAGE *(When Data Entered)*

404 992

20.

tion and a conventional factor group analysis. In general, these data lead to four essential conclusions concerning hexafluoride crystals: a) Fermi resonance plays an important role in producing the observed energy and intensity differences in this series; b) $\underline{k} = 0$ exciton structures are remarkably similar in the three crystals; c) similarities and differences between these solids can be directly correlated with molecular parameters such as dipole derivatives, polarizabilities, etc.; and d) phonons (external modes) can be neatly separated into rotational and translational normal modes.

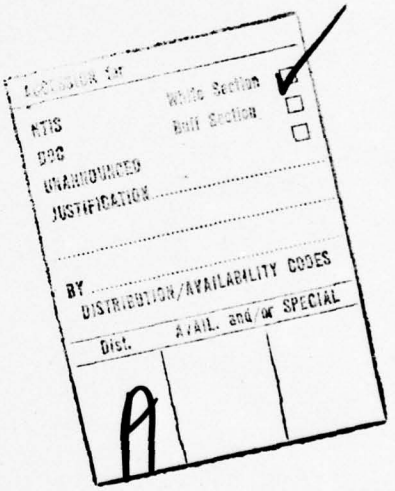

Abstract

Neat crystal Raman spectra of orthorhombic MoF_6, WF_6, and UF_6 are presented and discussed. This work lays the foundation for presentation of two-particle and total band structures in the two following papers. The neat crystal spectra are interpreted in terms of an internal-external mode separation and a conventional factor group analysis. In general, these data lead to four essential conclusions concerning hexafluoride crystals: a) Fermi resonance plays an important role in producing the observed energy and intensity differences in this series; b) $\underline{k} = 0$ exciton structures are remarkably similar in the three crystals; c) similarities and differences between these solids can be directly correlated with molecular parameters such as dipole derivatives, polarizabilities, etc.; and d) phonons (external modes) can be neatly separated into rotational and translational normal modes.

I. INTRODUCTION

The vibrational properties of the series of hexafluoride molecules have been extensively studied both theoretically and experimentally.[1] The octahedral structure makes this series a textbook example of vibrational analysis (for those compounds not subject to Jahn-Teller instability). With the development of narrow line tunable diode lasers, even the disadvantage of the relatively high molecular moment of inertia (closely spaced rotational structure) has to a large extent been overcome.[2] With the use of noble gas ion lasers in Raman spectroscopy more and finer details of the spectra have been observed.[3,4,5,6] Coupled with these experimental advances the determination of accurate potential functions containing various interactions has progressed markedly.[4,5,6,7]

Aside from the interest in the molecular properties, there have been few studies of the vibrational characteristics of these systems in condensed phases. Perhaps the sparcity of solid state investigations has been due to the experimental difficulties inherent in these systems. Of the studies in the literature, one made no attempt to understand the details of the solid, even to the point of discussing the factor group,[8] another explained large splittings of the UF_6 crystal vibrational spectra solely in terms of site effects,[9] and a third attempted to analyze vibrational relaxation rates in the solid from lineshapes ignoring the excitonic contributions to the structure.[10]

During the investigation of electronic transitions of ReF_6[11] in various MF_6 (M = Re, Mo, W, U) crystals, it became apparent that vibrational levels of these molecules evidence substantial exciton couplings. Additionally, two-particle transitions were observed in the ReF_6 vibronic structure. These

transitions have also been observed in IrF_6 spectra.[12] To begin to understand the nature of the crystal interactions we have initiated a study of the purely vibrational properties of the closed shell transition metal hexafluoride crystals. Besides corroborating the details of the two-particle transitions we hope to determine parameters of the exciton bands and make comments about the nature of the intermolecular potentials.

In order to keep any one part of this discussion of the crystal vibrational spectra of transition metal hexafluorides from becoming too cumbersome, we have chosen to divide the presentation into three separate papers. In this paper the low temperature neat crystal Raman spectra of UF_6, WF_6 and MoF_6 will be presented and discussed in terms of simple factor group analyses. The starting point for this analysis employs the octahedral normal modes of the molecules as a basis. Neat crystal phonon spectra have also been observed and characterized for these systems. In the following two papers we will discuss exciton density of states functions (from two-particle and mixed crystal spectra) and total band structures for Mo, W, and UF_6 crystals.

II. THEORETICAL

The description of the normal modes of an octahedral MF_6 molecule is almost completely determined by symmetry. The six modes consist of three stretching and three bending modes ordered as ν_1 through ν_6 and belonging (in order) to the irreducible representations a_{1g}, e_g, $2t_{1u}$, t_{2g}, and t_{2u}. The exact description of ν_3 and ν_4 depends on the details of the potential functions which determine the amount of mixing of the pure stretching and bending modes. For UF_6 the separation is nearly complete.[13] The simple symmetry predictions are that ν_1, ν_3, and ν_5 will be active in Raman scattering, ν_3 and ν_4 will be active in infrared absorption and ν_6 will be inactive.

The low temperature crystal structure of the hexafluorides belongs to the space group Pnma (D_{2h}^{16}). There are four molecules per unit cell at sites of C_s symmetry. The molecular geometry of UF_6 is approximately D_{4h}[11], but MoF_6 and WF_6 seem to be closer to O_h symmetry.

In the standard molecular crystals description of crystal energy levels (first order Frenkel model) each molecular excited state function becomes the basis for a band of N crystal states (N is the number of molecules in the crystal).[14] With four molecules per unit cell this band will have N/4 wave-vector ($\underline{k}$) values and four energies for each $\underline{k}$. Since optical processes in crystals have the approximate selection rule $\Delta\underline{k} = 0$, and since at this point we are considering excitations from the idealized zero degree $\underline{k} = 0$ ground state (or alternatively excitations which do not interact with existing thermally populated excitations of the crystal), only the $\underline{k} = 0$ states are of interest. The group theoretical description of these states is a simple exercise in factor group analysis.

By reducing the molecular symmetry to that of the appropriate C_s (site) subgroup of O_h, correlating the irreducible representations of these groups, and correlating the irreducible representations of the site and factor groups (Figure 1), one may obtain the factor group description of the four $\underline{k} = 0$ crystal functions induced by one molecular excited state function. Similarly, one may deduce the irreducible representations of the phonons by the analogous subduction and induction starting with the molecular description of translational and rotational vectors. The results are summarized in Table 1.

Besides the $\underline{k} = 0$ selection rule for Raman scattering there is also an inversion parity rule. Only gerade states may be created in the crystal from the gerade ground state. Since every site irreducible representation induces two gerade and two ungerade factor group irreducible representations, $2m$ $\underline{k} = 0$ transitions are expected in the Raman spectra of these crystals in the energy region of a molecular vibration wtih degeneracy m. Likewise, treating rotations and translations of the whole molecule, twelve $\underline{k} = 0$ optical phonon peaks are expected in the Raman spectra.

A very interesting consequence of the C_s site symmetry is that all molecular vibrations generate Raman allowed factor group states regardless of the free molecule inversion characteristics of the vibrations. Furthermore, since states of the same symmetry may mix in the crystal, the optical phonons are theoretically expected to be mixed translational and librational motions even at $\underline{k} = 0$.

III. REVIEW OF THE VAPOR PHASE RAMAN SPECTRA

Laser Raman spectra of all of the stable, nonphotosensitive hexafluorides have recently been published.[3] In the normal (non Jahn-Teller) compounds, the spectra are quite simple. An intense polarized high energy peak with two weaker depolarized lower energy peaks are the main features. These were assigned as the ν_1, ν_2 and ν_5 fundamentals. Also some very weak peaks were assigned as combinations and overtones. The strongest of these is the 2 ν_6 feature. While one might be tempted to consider this a Fermi resonance effect, the correlation of the 2 ν_6 distance from ν_5 and the 2 ν_6 intensities relative to ν_5 are not completely systematic. Differences in details of anharmonicities and second order polarizability tensor terms may be responsible for this lack of correlation.

IV. EXPERIMENTAL

The details of the experimental procedures and apparatus are by now well known. Briefly, though, samples were prepared in monel vacuum lines and loaded into small Pyrex cells of various shapes which were attached to the monel system. Single crystals were grown from the vapor over periods of many weeks at temperatures below the cubic-orthorhombic solid-solid phase transitions. UF_6 crystals were grown at room temperature as they do not exhibit the transition. Crystals were slowly cooled by lowering them into liquid nitrogen. Samples were then supported inside a small Pyrex dewar and spectra were obtained.

The Raman spectra were obtained on three different laser Raman spectrometers. Since high resolution and wavelength accuracy became important for the investigations, the final data were obtained on a system utilizing diffraction limited optics and micropositioning mounts in conjunction with an f/5.8 0.5m double monochromator designed to minimize tracking errors. The monochromator was calibrated throughout the range of Raman scattering with approximately 600 Fe-Ne hollow cathode lines using a correction expression devised to incorporate drive screw cam effects. Raman spectra were obtained in second order of a 1200 g/mm grating using the 5145Å Ar^+ laser line (1-2 watts). The standard deviation for one measurement in the calibration fit was less than 0.1Å; absolute frequency accuracy to better than 0.2 cm^{-1} can be expected. Reproducibility of sharp peaks was frequently seen to be in hundredths of cm^{-1}. It should be noted, though, that the laser was not run with an etalon and the typical 0.15 cm^{-1} width of Ar^+ laser lines may be a practical limitation of the total accuracy (and observable linewidths).

V. RESULTS AND DISCUSSION

Tables 2, 3, and 4 list the observed Raman spectral features of the MoF_6, WF_6, and UF_6 (77K) crystals along with the assignments in terms of the molecular (O_h) vibrations. Representative spectra are displayed in Figures 2 through 8. It should be mentioned that no significant orientation (polarization) effects have been observed. The single minor exception to this generalization is a weak doublet in the ν_3 region of UF_6. The absence of orientation-dependent spectra, even though the laser output was polarized and single crystals were employed in these studies, is probably associated with beam convergence in a randomly oriented biaxial crystal.

The general features of the spectra can be explained in terms of the internal and external vibrations of the molecular entities constituting the crystals. The internal vibrations with a few exceptions are easily associated with the normal coordinates of the octahedral molecules, modified only slightly by the reduced molecular (site) symmetry. The external vibrations appear to be well separated from the internal motions and have been tentatively assigned in terms of an idealized phonon translation and rotation (libration) separation.

A. Internal Vibrations

Low resolution survey spectra of the fundamental regions are displayed in Figure 2. In these logarithmic traces the totally symmetric ν_1 peak is typically greater than 10^5 cps while the background is less than 10^2 cps. The identification of groupings of features in terms of molecular vibrations follows from the gas phase spectra. The ν_1, ν_2, and ν_5 fundamentals and the 2 ν_6 peaks are in the same regions as in the published spectra. The weaker ν_3 and ν_4 features observed due to loss of molecular inversion symmetry are centered around

the frequencies derived from infrared data. The ν_6 features, visible in these traces only for UF_6, are observed directly here for the first time. As explained in Section II, only $\underline{k} = 0$ components of the bands derived from the fundamental levels are observed.

The ν_1 feature is in all three cases one apparently symmetric peak with width less than 1 cm^{-1}. It is sometimes limited by the monochromator resolving power and laser linewidth. No indication has been seen of the splitting of the A_g and B_{2g} factor group components. This is in keeping with a general view of excitonic interactions as electrostatic multipolar interactions. The lowest multipole sustained by a neutral octahedral molecule is a hexadecapole. Quite likely, the crystal induced lower moments would give even larger interactions than this hexadecapole-hexadecapole term.

Figure 3 shows the ν_2 regions of these crystals at high resolution. The four features in UF_6 and MoF_6 are seen to be quite similar when the energy scales are shifted and normalized. The four components are undoubtedly the A_g, B_{1g}, B_{2g}, and B_{3g} factor group components. The appearance of five features in the WF_6 spectrum is a consequence of the nearness of the ν_3 fundamental (711 cm^{-1} in the vapor)[3] and of the large bandwidth of that mode (see below). These circumstances create an extra peak due to overlapping bands. The identification of features deriving from solely ν_2 or ν_3 is not possible when the bands overlap. It is, however, tempting to suggest that the bands at ca. 678 cm^{-1} are associated with the ν_2-ν_3 interaction and the features between 675 and 668 cm^{-1} are mostly of ν_2 character.

In the ν_5 region (Figure 4) the UF_6 spectrum displays five of the predicted six components. The WF_6 and MoF_6 spectra suggest more than three features because of the inflections and linewidths. Again, the great similarity of these spectra is apparent when the energy scales are shifted and normal-

ized. As for the ν_2 band, the structure in UF_6 is about twice as large as in WF_6 and MoF_6. The greater polarizability of UF_6 with respect to the other two compounds (inferred from the ordering of the lowest charge transfer transitions of the molecules) has probably an important role in determining this. It is interesting to note that the ordering of the vibrational frequencies follows these same systematics.

The ν_3 regions are displayed in Figure 5. Recalling that ν_3 overlaps with the ν_2 band in WF_6 the similarity of the other two bands again stands out. There is interference by the intense totally symmetric transition at high energy; however, the observation of five peaks in the UF_6 spectrum nearly fulfills the factor group prediction. It is likely that the high energy component in MoF_6 similar to that in UF_6 is buried under the ν_1 peak. In the octahedral molecule this mode is electric dipole allowed. Again, invoking multipolar excitonic interactions it is not surprising that this band exhibits the largest spread of $\underline{k} = 0$ components.

The ν_4 and ν_6 bands are most intense in UF_6 crystals (Figure 6). Their proximity to the ν_5 band suggests a crystal induced Fermi resonance mechanism is responsible for the observed enhancement with respect to MoF_6 and WF_6 transitions. UF_6 molecules are also more distorted in the solid than are MoF_6 molecules and this lower symmetry could additionally generate more intensity in the ν_4 and ν_6 transitions. However, the similar intensities in the ν_3 regions of these crystals and the greater intensity of ν_4 (closer to ν_5) over ν_6 in all crystals argues for the importance of a Fermi resonance mechanism.

Not all predicted components were observed in this region. Some may be masked by the ν_5 band and some may not be resolved since relatively wide slits were necessary to obtain measurable signals. In MoF_6 and WF_6 the ν_4-ν_6 regions are too weak to be of much additional value over and above the previously reported two-

particle ReF_6-MF_6 vibronic transitions[11] for the 2 ν_6 peaks discussed below.

B. Combinations and Overtones of Internal Modes

Various weak features corresponding to combinations and overtones of the internal vibrational modes have been observed. Figure 7 shows the region between the intense ν_5 and ν_2 features in the UF_6 and MoF_6 crystals. Discussion of these bands in terms of crystal states is rather involved. Besides the crystal states that could be derived from the molecular combination or overtone levels (single particle states), there are crystal states corresponding to the creation of the individual vibrations on separate molecules (two-particle states). The observation of broad bands without sharp features is an indication of two-particle character. $\underline{k} = 0$ selection rules can be satisfied by states created from the convolution of two bands in the latter situation. The number of such states is approximately equal to the number of molecules in the crystal. This result is quite different from the one predicted by a factor group analysis for single particle states. Expectations for this latter case would indicate relatively few sharp, well-separated features. As with all neat crystal $\underline{k} = 0$ structures, the center of gravity of the observed two-particle structure need not (and in general does not) fall at the frequency of the band center. This area will be covered in more detail in the following paper.

C. External Modes

Figure 8 displays the energy region below the lowest internal mode. This portion of the spectrum of neat crystal ReF_6 at 77K has been added to aid in the assignment of the features. As discussed in Section II and summarized in Table 1, there will be 12 Raman allowed $\underline{k} = 0$ phonons. While formally they may be mixtures of translational and librational modes, there is some indi-

cation that the mixing is not severe. Since the phonon sideband structure observed in the 2 mμ absorption spectrum of ReF_6 doped into these crystals is quite similar to the observed $\underline{k} = 0$ grouping of phonons, the dispersion is probably not large, as is expected for optical phonon branches. If this is true, it is probably also true that translation-libration mixing will not be important at $\underline{k} = 0$, unless the same symmetry translation and libration states are close in energy.

To test this hypothesis consider the following model for the external modes based on the idea that all of these molecules "look" nearly identical from the exterior. Harmonic oscillator (phonon) frequencies are given by $(k/m)^{\frac{1}{2}}/2\pi$ in which k is the force constant and m is the reduced mass for the motion. If it is assumed that the force constants for and descriptions of each normal mode remain unchanged from crystal to crystal and that the external motions are either pure translation or pure rotation (the reduced masses are thereby proportional to the molecular weight M or the molecular moments of inertia I), then letting i index the phonon mode,

$$m_i = A_i M$$

or

$$m_i = A_i I.$$

The observed frequencies will then be directly proportional to either $M^{-\frac{1}{2}}$ or $I^{-\frac{1}{2}}$.

$$\nu_i = [k_i/4\pi^2 A_i]^{\frac{1}{2}} M^{-\frac{1}{2}}$$

or

$$\nu_i = [k_i/4\pi^2 A_i]^{\frac{1}{2}} I^{-\frac{1}{2}} \qquad (1)$$

Figure 9 displays the observed frequencies plotted in this manner. Various lines indicate a particular phonon motion.

A few words should be said about the determination of moments of inertia. The recent neutron diffraction data for MoF_6 and UF_6 were examined to determine the displacement of the central metal from the center of mass of the fluoride

atoms. In MoF_6 the displacement was identically zero while in UF_6 the displacement was .073 A in the c direction. This value was well below the accumulated errors, so the uranium atom has been treated as if it were at the center of mass. Table 5 is a listing of the parameters used, assuming isotropic moment of inertia tensors.

It was possible with a choice of twelve phonon modes to fit all but two observed peaks. The 18.4 cm^{-1} state in ReF_6 is probably perturbed by the low energy electronic exciton band and the isolated occurrence of the 89.8 cm^{-1} peak in UF_6 is unexplained. Two of the phonons were not clearly identified as translational or librational since they fit into either graph. It would be interesting to test this assignment with polarization studies to prove the similar mode properties within each series. These data are summarized in Table 6. The model can be seen, however, to be an appropriate description of the phonon modes in this series of crystals.

One might be tempted to utilize the isotope product and sum rules to help identify the phonons. But, in fact, it is exactly the generalization of the conservation of force constants and description of motions to complete irreducible representations (rather than each individual motion as done here) which forms the basis of that technique. No new information can be gained since product and sum rules are automatically satisfied for any combination of these phonon series. More explicitly for <u>any</u> combination of phonons the ratio of products of frequencies between crystals is (i labels translational and j labels librational phonons),

$$\left\{\prod_i \frac{(\nu_i)^2_{MF_6}}{(\nu_i)^2_{M'F_6}}\right\}\left\{\prod_j \frac{(\nu_j)^2_{MF_6}}{(\nu_j)^2_{M'F_6}}\right\} = \left\{\prod_i \frac{k_i/A_i(M)_{MF_6}}{k_i/A_i(M)_{M'F_6}}\right\}\left\{\prod_j \frac{k_j/A_j(I)_{MF_6}}{k_j/A_j(I)_{M'F_6}}\right\} =$$

$$\left[\frac{(M)_{M'F_6}}{(M)_{MF_6}}\right]^{n_i} \left[\frac{(I)_{M'F_6}}{(I)_{MF_6}}\right]^{n_j},$$

in which there are n_i and n_j terms in the respective products.

This is exactly the product rule which is required to hold for all modes belonging to one irreducible representation. Such an expression is only useful when it fails to hold for the other combinations of vibrations. These relations are valid, of course, because of the highly restrictive nature of equations 1.

VI. SUMMARY

Raman spectra of neat crystals of MoF_6, WF_6 and UF_6 have been obtained and discussed in terms of the internal and external modes of the molecules. The spectra of the fundamental regions are consistent with factor group predictions based on the published crystal structures. Molecular and crystal Fermi resonances are important in understanding differences between the various crystal spectra and for explaining intensity distributions. The excitonic structures are remarkably alike when energy scales are normalized for each fundamental region. The similarity is a crystal phenomena and the energy scaling is attributed to differences in molecular properties (e.g., polarizability and electric dipole derivatives). The external modes have been fit to a model treating the optical phonons as crystal independent pure translational and librational normal modes.

1. G. L. Goodman and B. Weinstock, Adv. Chem. Phys. 9, 169 (1965).

2. J. P. Aldridge, H. Filip, H. Flicker, R. F. Holland, R. S. McDowell, N. G. Nereson and K. Fox, J. Mol. Spec. 58, 165 (1975).

3. H. H. Claassen, G. L. Goodman, J. H. Holloway and H. Selig, J. Chem. Phys. 53, 341 (1970).

4. R. S. McDowell, R. J. Sherman, L. B. Asprey and R. C. Kennedy, J. Chem. Phys. 62, 3974 (1975).

5. R. S. McDowell and L. B. Asprey, J. Mol. Spec. 48, 254 (1973).

6. R. S. McDowell, L. B. Asprey and R. T. Paine, J. Chem. Phys. 61, 3571 (1974).

7. K. Fox, B. J. Krohn and W. H. Shaffer, Paper RM11, *Thirty-First Symposium* on Molecular Spectroscopy (Ohio State University, Columbus, Ohio, June 14-18, 1976).

8. K. H. Hellberg, A. Muller and O. Glemsen, Z. Natur. 21b, 118 (1966).

9. R. Bougon and P. Rigny, C. R. Acad. Sci. Paris C263, 1321 (1966).

10. M. Gilbert and M. Drifford, in Advances in Raman Spectroscopy, ed. by J. P. Mathieu (Heydon and Sons, New York, 1973), page 204.

11. E. R. Bernstein and G. R. Meredith, J. Chem. Phys. 64, 375 (1976).

12. J. D. Webb, unpublished results.

13. R. S. McDowell, Los Alamos Scientific Laboratory Internal Document CNC-3-75:18 (May 1, 1975).

14. R. Kopelman, Excited States, Ed. by E.C. Lim(Academic Press, 1975), Vol. II, page 34ff.

Table 1. Summary of Factor Group Predictions for Transition Metal Hexafluoride Orthorhombic Structure (Pnma)

Molecular Mode	O_h Irreducible Representations	C_s Irreducible Representations		D_{2h} (Factor Group) Irreducible Representations							
		A'	A"	A_g	B_{1g}	B_{2g}	B_{3g}	A_u	B_{1u}	B_{2u}	B_{3u}
Translation	T_{1u}	2	1	2	1	2	1	1	2	1	2
Rotation	T_{1g}	1	2	1	2	1	2	2	1	2	1
ν_1	A_{1g}	1	0	1	0	1	0	0	1	0	1
ν_2	E_g	1	1	1	1	1	1	1	1	1	1
ν_3	T_{1u}	2	1	2	1	2	1	1	2	1	2
ν_4	T_{1u}	2	1	2	1	2	1	1	2	1	2
ν_5	T_{2g}	2	1	2	1	2	1	1	2	1	2
ν_6	T_{2u}	1	2	1	2	1	2	2	1	2	1

Table 2. Summary of Neat MoF_6 Crystal Raman Spectra at 77K.

Stokes Shift (cm^{-1})	FWHH (cm^{-1})	Assignment	Stokes Shift (cm^{-1})	FWHH (cm^{-1})	Assignment
30.9			642.43	.8	
36.4			645.12	1.2	ν_2
40.7			645.62		
59.6		phonons	652.45	.8	
66.6			694.60	1.2	
72.7			702.63	1.9	ν_3
82.7			718.73	2.0	
128			721.64		
140		ν_6	742.19	<.3	ν_1
247.62	<1.5		816.9	40	
252.34	1.1				
261.87	1.0	ν_4	927.1	38	$\nu_2 + 2\nu_6$
267.25			967.8		$\nu_2 + \nu_5$
272.08					
275.81	20		1061.8	10	$\nu_1 + \nu_5$
278.20		$2\nu_6$	1289.0	7.3	$2\nu_2$
316.02			1385.59	14	$\nu_1 + \nu_2$
319.50	3.1	ν_5	1392.91		
324.78	2.1		1482.79	1.2	$2\nu_1$
378.3		$\nu_4 + \nu_6$			
395.4	36				
412.5		$3\nu_6$			
454.3		$\nu_5 + \nu_6$			
498.9					
526.3	11	$2\nu_4$			
548.6		$4\nu_6$			
585.6	32	$\nu_4 + \nu_5$			

Table 3. Summary of Neat WF_6 Crystal Raman Spectra at 77K.

Stokes Shift (cm^{-1})	FWHH (cm^{-1})	Assignment	Stokes Shift (cm^{-1})	FWHH (cm^{-1})	Assignment
26.0			669.16	.5	
30.7			672.17	.4	ν_2
35.5			673.62	.4	
65.5		phonons	675.60	.4	
72.4			678.89	.5	
76.5			692.70	.6	ν_3
84.4			698.48	.6	
115			772.25	<.3	ν_1
147		ν_6	816.1		
240.11	<3		828.3		
249.87	<3	ν_4			
265.85	<3		1058.2	5.2	$\nu_1 + 2\nu_6$
291.4	22	$2\nu_6$	1094.7	10.4	$\nu_1 + \nu_5$
320.35			1342		$2\nu_2$
323.66	2.6	ν_5	1385		$2\nu_3$
328.31	3.5		1443		$\nu_1 + \nu_2$
388		$\nu_4 + \nu_6$	1542.49	<1.8	$2\nu_1$
465		$2\nu_4, \nu_5+\nu_6$	1552.72		
607		$\nu_4 + \nu_5$			
650		$2\nu_5$			

Table 4. Summary of Neat UF_6 Crystal Raman Spectra at 77K.

Stokes Shift (cm^{-1})	FWHH (cm^{-1})	Assignment	Stokes Shift (cm^{-1})	FWHH (cm^{-1})	Assignment
28.4			510.80	.4	
34.6			516.89	.35	
47.0			518.29	.4	ν_2
72.5		phonons	534.36	.5	
77.8			586.39		
89.8			590.06		
103.2			608.43		ν_3
145.82	1.9		610.74		
149.03	2.4		649.08		
155.27	2.2	ν_6	663.96	.5	ν_1
163.25	2.8		700.3		
175.33	2.1		718.2		$\nu_2 + \nu_5$
185.83	1.4		752.1		ν_1 (ReF_6)?
191.64	1.2	ν_4	819.4	29	$\nu_1 + \nu_6$
197.18			870.15		
206.73	1.3		877.12		$\nu_1 + \nu_5$
211.22	1.1		887.37		
215.65	1.6	ν_5	1035.97	54	$2\nu_2$
226.12	1.8		1181.47	30	$\nu_1 + \nu_2, 2\nu_3$
229.64			1327.96	1.6	$2\nu_1$
308.4	22	$2\nu_6$			
335.7		$\nu_4 + \nu_6$			
374.8	41	$2\nu_4, \nu_5+\nu_6$			
399.6		$\nu_4 + \nu_5$			
426.0	36	$2\nu_5$			
452.3					
470.0					
491.8					

Table 5. Summary of Molecular Parameters Used to Evaluate Phonon Modes.

	M-F Distance (A°)				
Molecule	Electron Diffraction	Crystal Structure	Adopted Value	Moment of Inertia (amu·A^2)	Molecular Weight (amu)
MoF_6	1.820	1.809	1.81	249.0	209.9
WF_6	1.833		1.83	254.5	297.9
ReF_6	1.832		1.83	254.5	300.2
UF_6	1.996	1.97	1.97	294.9	352.0

Table 6. Summary of Phonon Assignments Based on the Analysis of Section V.C. Assignments L_i and T_i are based on Figure 9 and are indicated on the specific mode lines.

MoF_6		WF_6		ReF_6		UF_6	
Energy (cm^{-1})	Assignment	Energy (cm^{-1})	Assignment	Energy (cm^{-1})	Assignment	Energy (cm^{-1})	Assignment
30.9	L_1, T_1	26.0	T_1	18.4		28.4	L_1, T_2
36.4	L_2, T_2	30.7	L_1, T_2	25.6[a]	(T_1)	34.6	L_2, T_6
40.7	T_6	35.5	L_2, T_6	29.9	L_1, T_2	47.0	$L_7 = T_3$
59.6	T_3	65.5	L_3	35.4	L_2, T_6	72.5	$L_5 = T_7$
66.6	L_3	72.4	L_4	49.2	$L_7 = T_3$[b]	77.8	L_6, T_4
72.7	L_4	76.5	$L_5 = T_7$[b]	65.4	L_3	89.8	
82.7	L_6	84.4	L_6, T_4	82.9	L_6, T_4	103.2	T_5
128	T_5	115	T_5				

a. This peak also corresponds to a Raman transition to a low lying electronic state.

b. This phonon could be either a translational or librational motion based on Figure 9.

Figure 1. Correlation Diagrams Appropriate to the Vibrational Factor Group Analysis of Transition Metal Hexafluorides. The two's in the correlation from O_h to C_s irreducible representations indicate that the lower symmetry representation occurs twice.

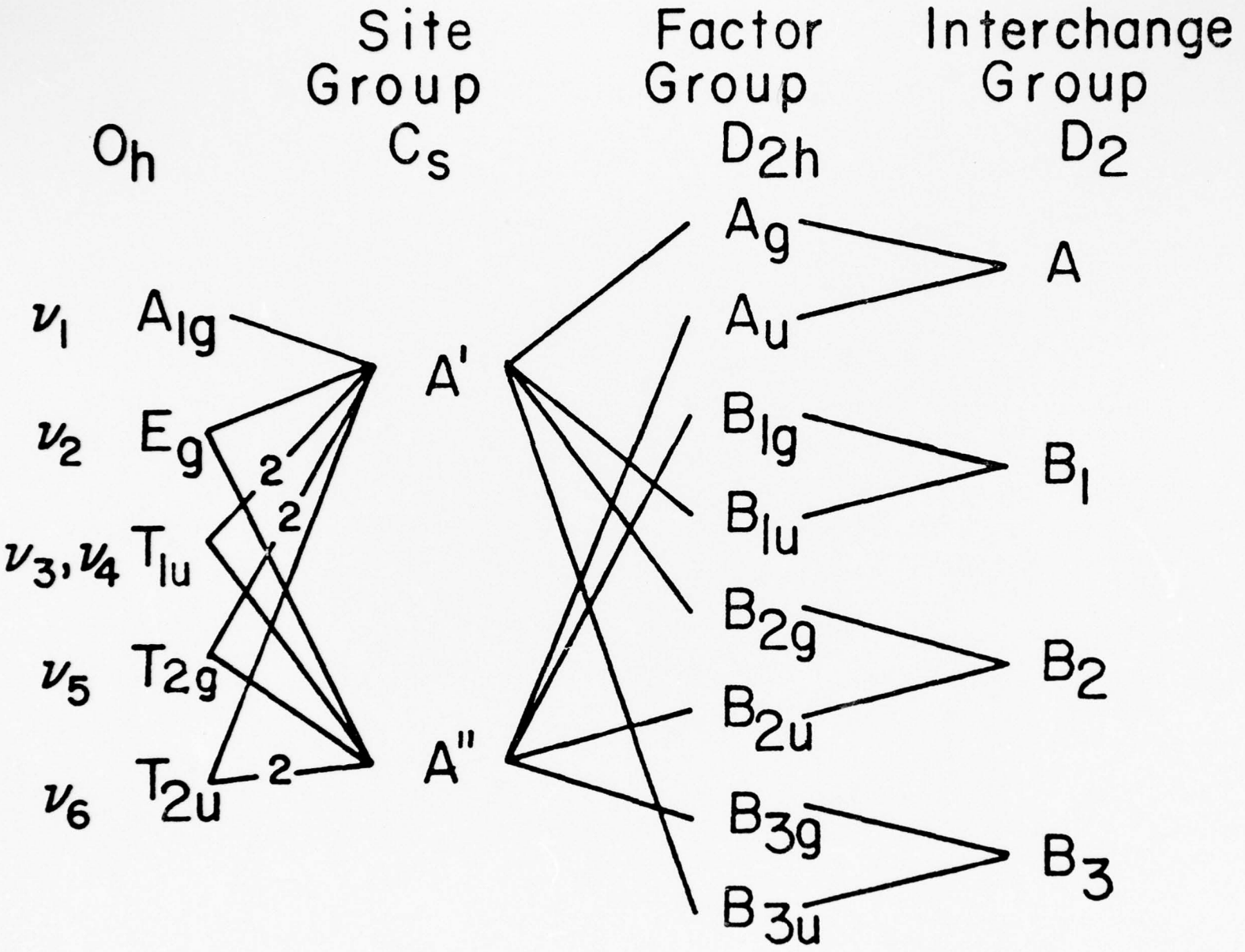
Site Group
Factor Group
Interchange Group
O_h
C_s
D_{2h}
D_2
ν_1 A_{1g}
ν_2 E_g
ν_3, ν_4 T_{1u}
ν_5 T_{2g}
ν_6 T_{2u}
2
2
2
A'
A''
A_g
A_u
B_{1g}
B_{1u}
B_{2g}
B_{2u}
B_{3g}
B_{3u}
A
B_1
B_2
B_3

Figure 2. Low Resolution Raman Spectra of Neat MoF_6, WF_6 and UF_6 Crystals Near 77K. The ordinate is a logarithmic scale. The baselines correspond to less than 100 cps while the ν_1 peaks are approximately 10^5 cps. The assignment of features can be readily seen in Tables 2, 3 and 4.

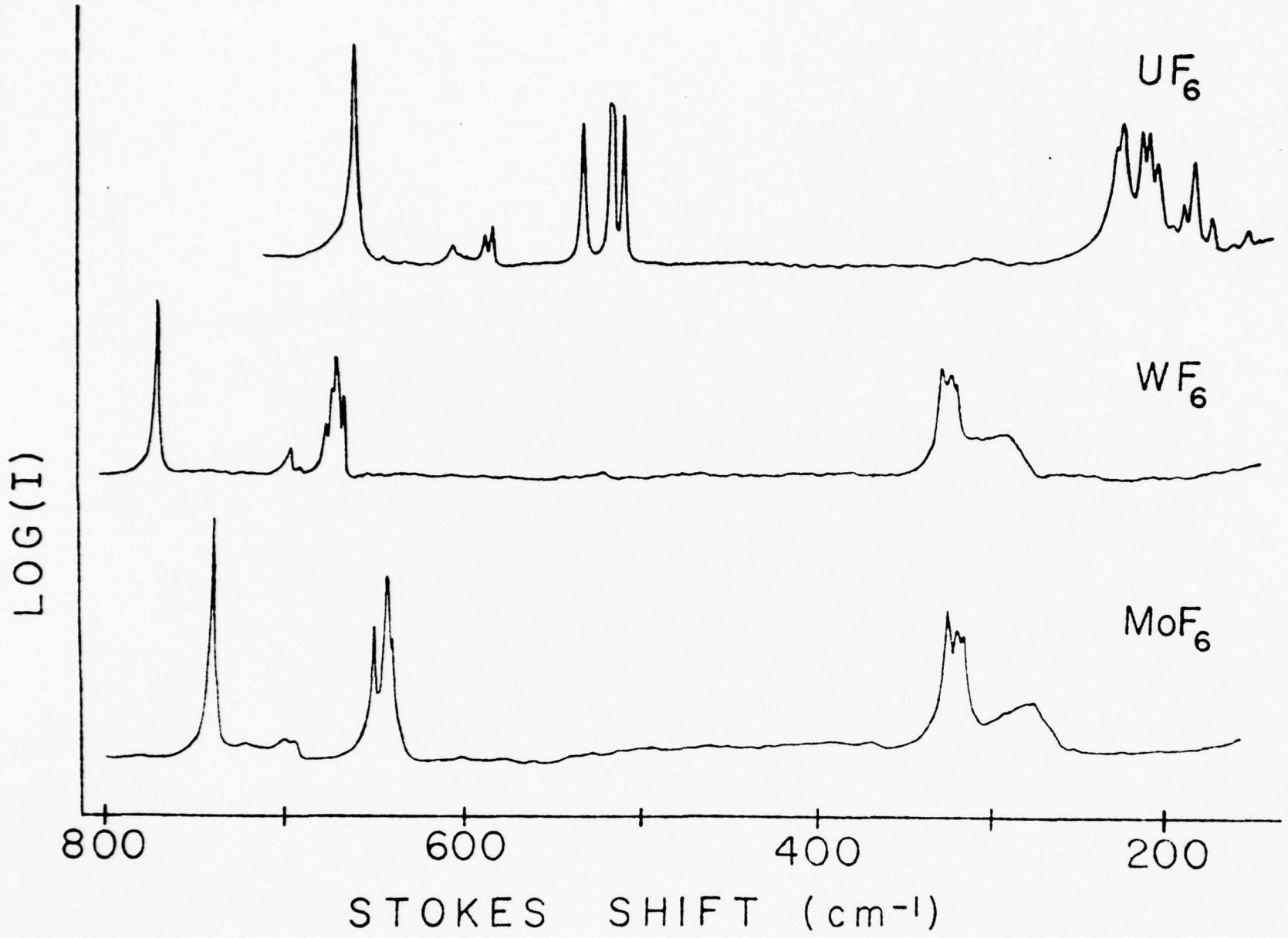
UF6
WF6
MoF6
LOG(I)
800
600
400
200
STOKES SHIFT (cm-1)

Figure 3. High Resolution Raman Spectra of the ν_2 Exciton Region of Neat MoF_6, WF_6 and UF_6 Crystals Near 77K. Notice that the scales have been shifted and normalized to point out the similarities of structure. The WF_6 spectrum is complicated due to the overlap of the ν_2 and ν_3 exciton bands (see text). The feature marked Ar^+ in the UF_6 spectrum is the 5287Å plasma line of the laser.

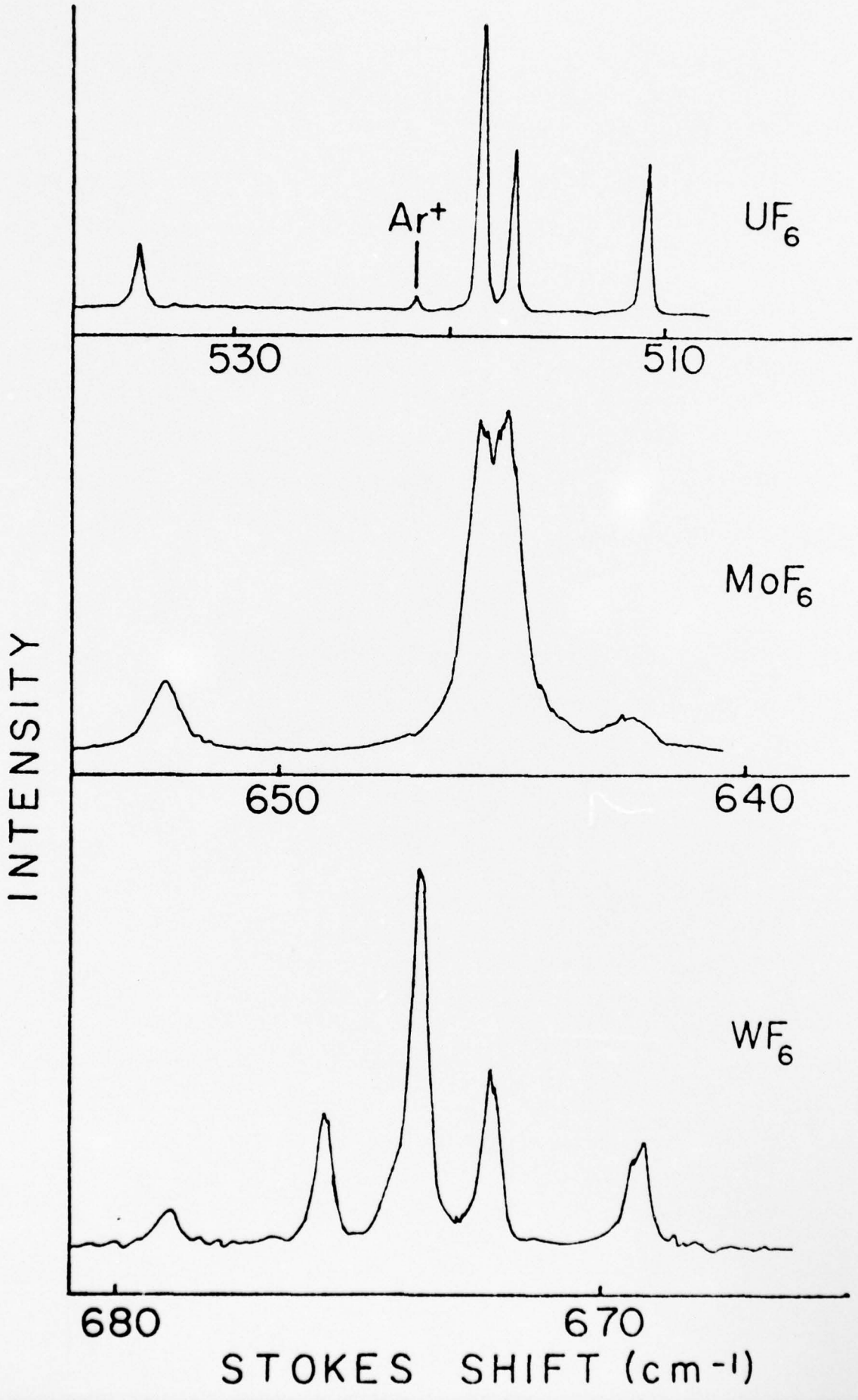
Ar+
UF6
530
510
MoF6
650
640
INTENSITY
WF6
680
670
STOKES SHIFT (cm-1)

Figure 4. High Resolution Raman Spectra of the ν_5 Exciton Region of Neat MoF_6, WF_6, and UF_6 Crystals Near 77K. The scales have been shifted and normalized to bring out the similarity of features.

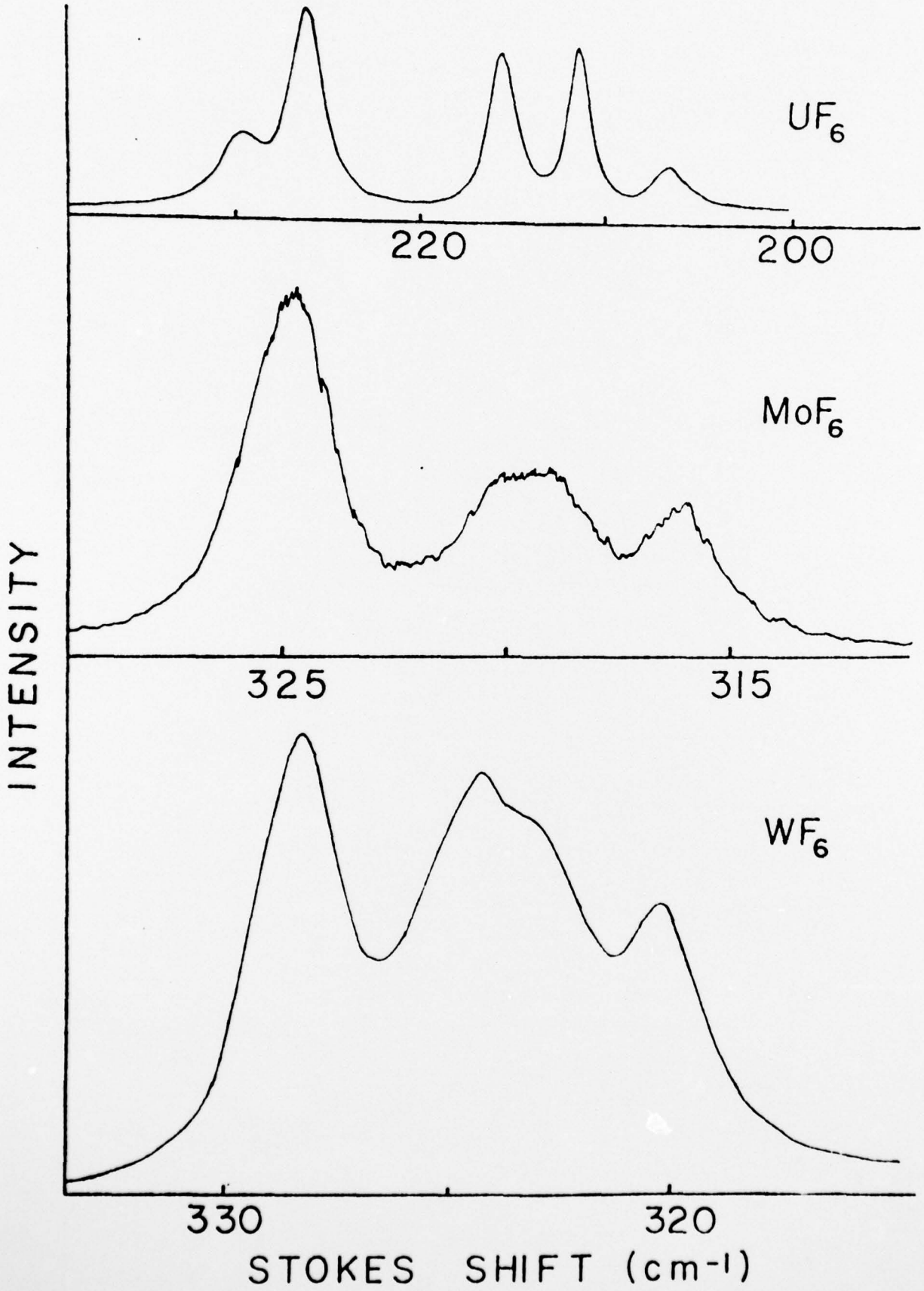
UF6
220
200
MoF6
325
315
WF6
330
320
INTENSITY
STOKES SHIFT (cm-1)

Figure 5. High Resolution Raman Spectra of the ν_3 Exciton Region of Neat Crystals Near 77K. A is UF_6 and B is MoF_6. The WF_6 spectrum has been omitted because of the absence of readily identifiable ν_3 structure due to the overlap with the ν_2 exciton band. The high energy feature (ca. 650 cm^{-1}) in UF_6 is included in the exciton band based on a comparison with the ν_3 and $\nu_1 + \nu_3$ infrared absorption spectra of reference 9. Similar slits and powers were used as those used to obtain the other portion of the spectrum.

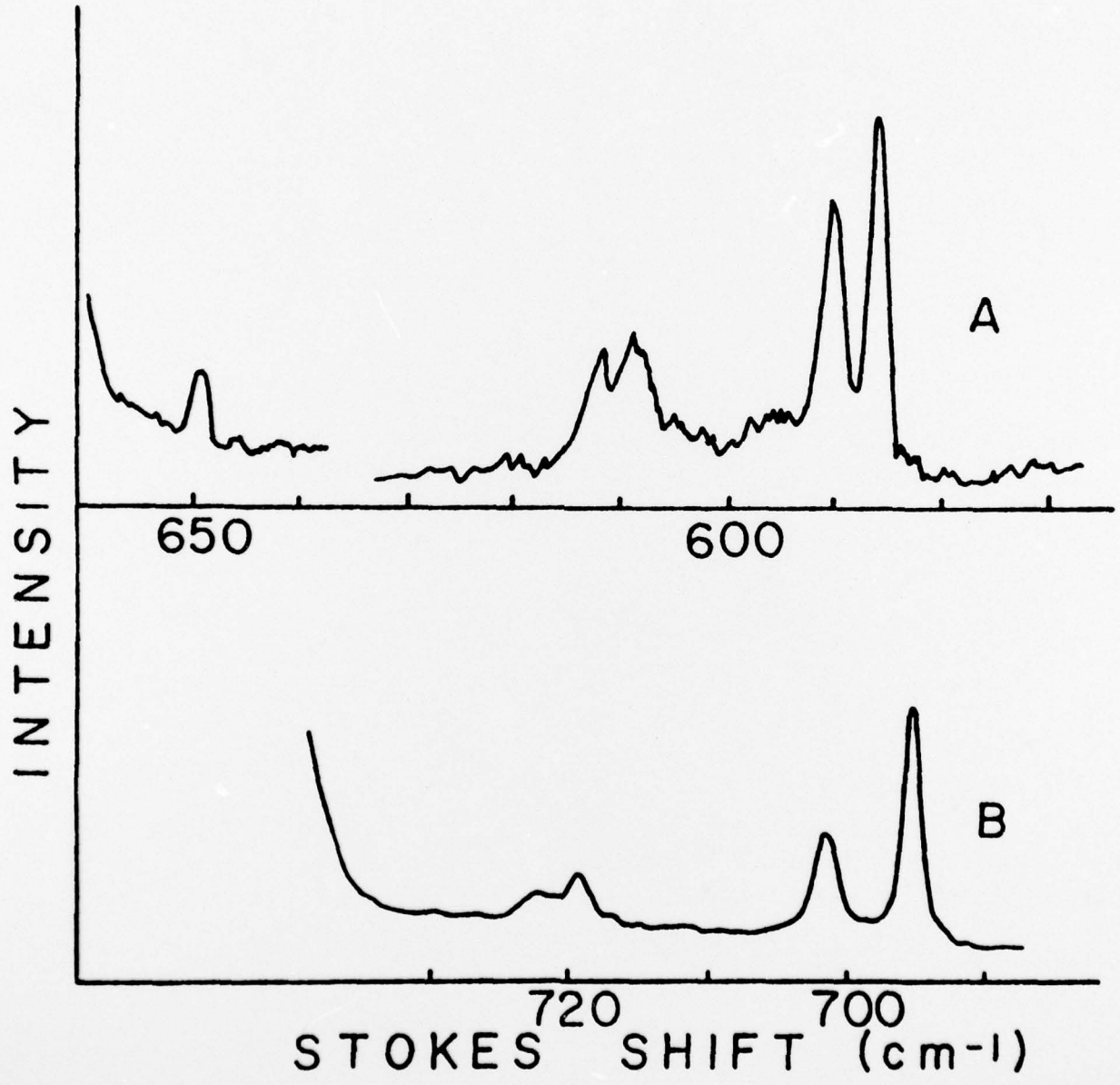
INTENSITY
650
600
A
720
700
B
STOKES SHIFT (cm-1)

Figure 6. Medium Resolution Spectra of the ν_6 (140-170 cm^{-1}) and ν_4 (180-200 cm^{-1}) Exciton Regions of Neat UF_6 Crystal Near 77K. The feature at 207 cm^{-1} has been assigned to ν_5. $I(\nu_5) >> I(\nu_4) > I(\nu_6)$. Some of the transitions of the ν_6 band may be masked by ν_4 intensity and some of the ν_4 transitions probably lie under the ν_5 intensity.

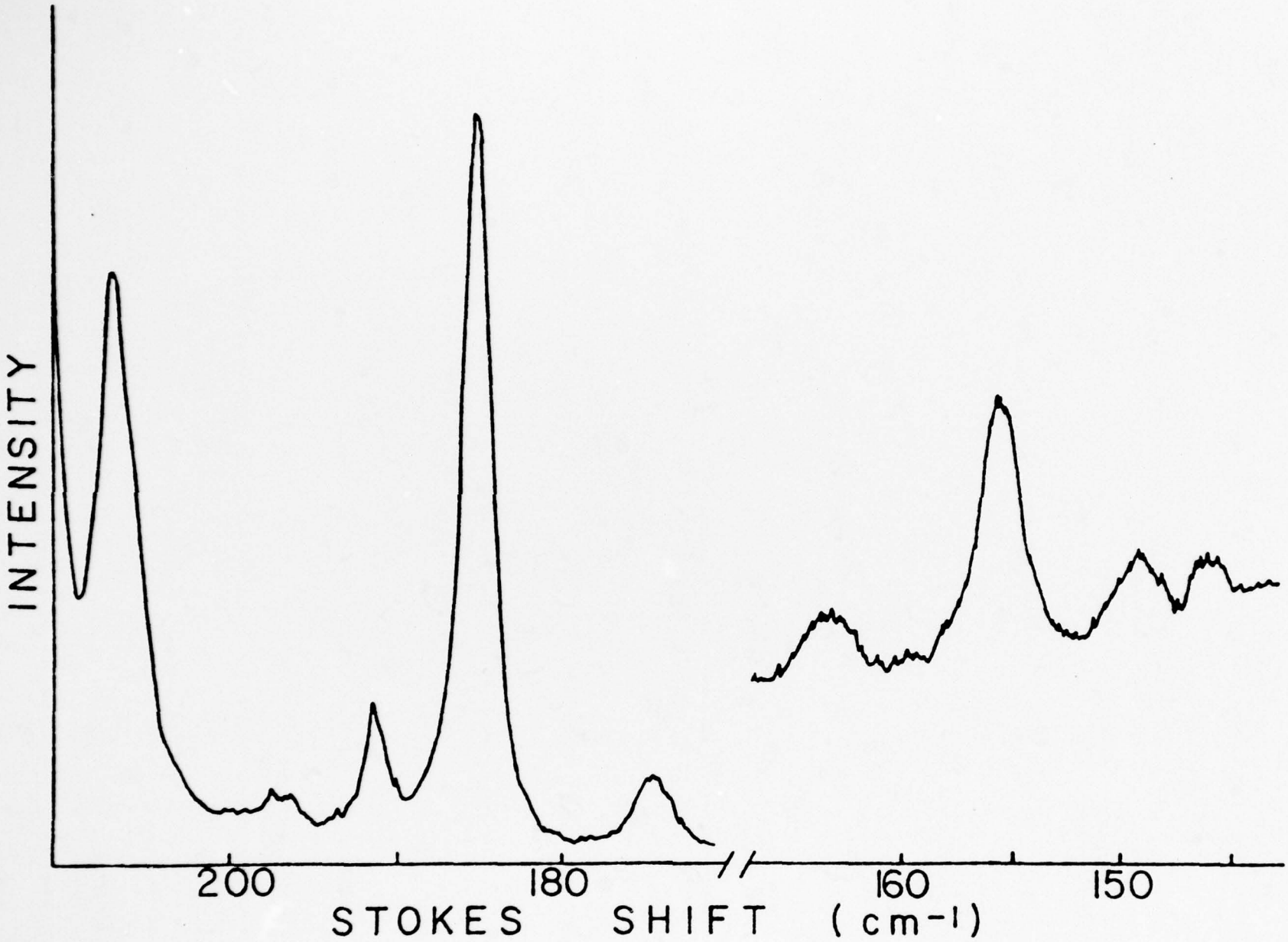
INTENSITY
200
180
160
150
STOKES SHIFT (cm-1)

Figure 7. Raman Spectra of the Bending Mode Combination and Overtone Regions in Neat Crystals Near 77K. A is UF_6 and B is MoF_6. No sharp features were observed in these regions indicating a high density of Raman active $\underline{k} = 0$ components.

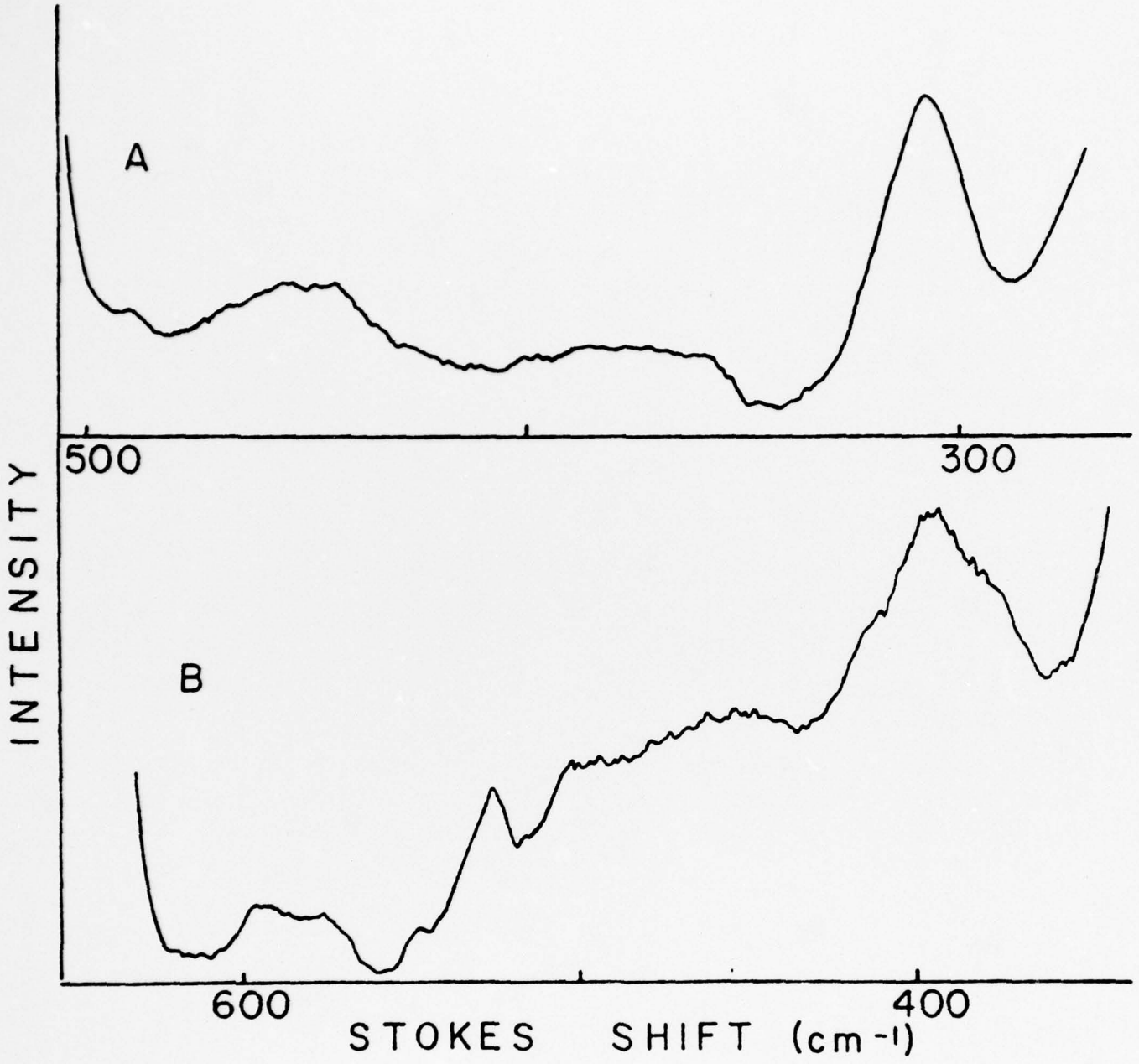
A
500
300
INTENSITY
B
600
400
STOKES SHIFT (cm-1)

Figure 8. Raman Spectra of the Phonon Region of Neat Crystals Near 77K. The key is:

a) MoF_6

b) WF_6

c) ReF_6

d) UF_6

The spectra are presented in this overlapping linear intensity manner to bring out the structure which is weak relative to the Rayleigh plus Brillouin scatter. The intense feature near 26 cm^{-1} in ReF_6 is electronic Raman scattering to the upper levels of the split $G_{3/2g}$ (Γ_8 fourfold degenerate) electronic ground state.

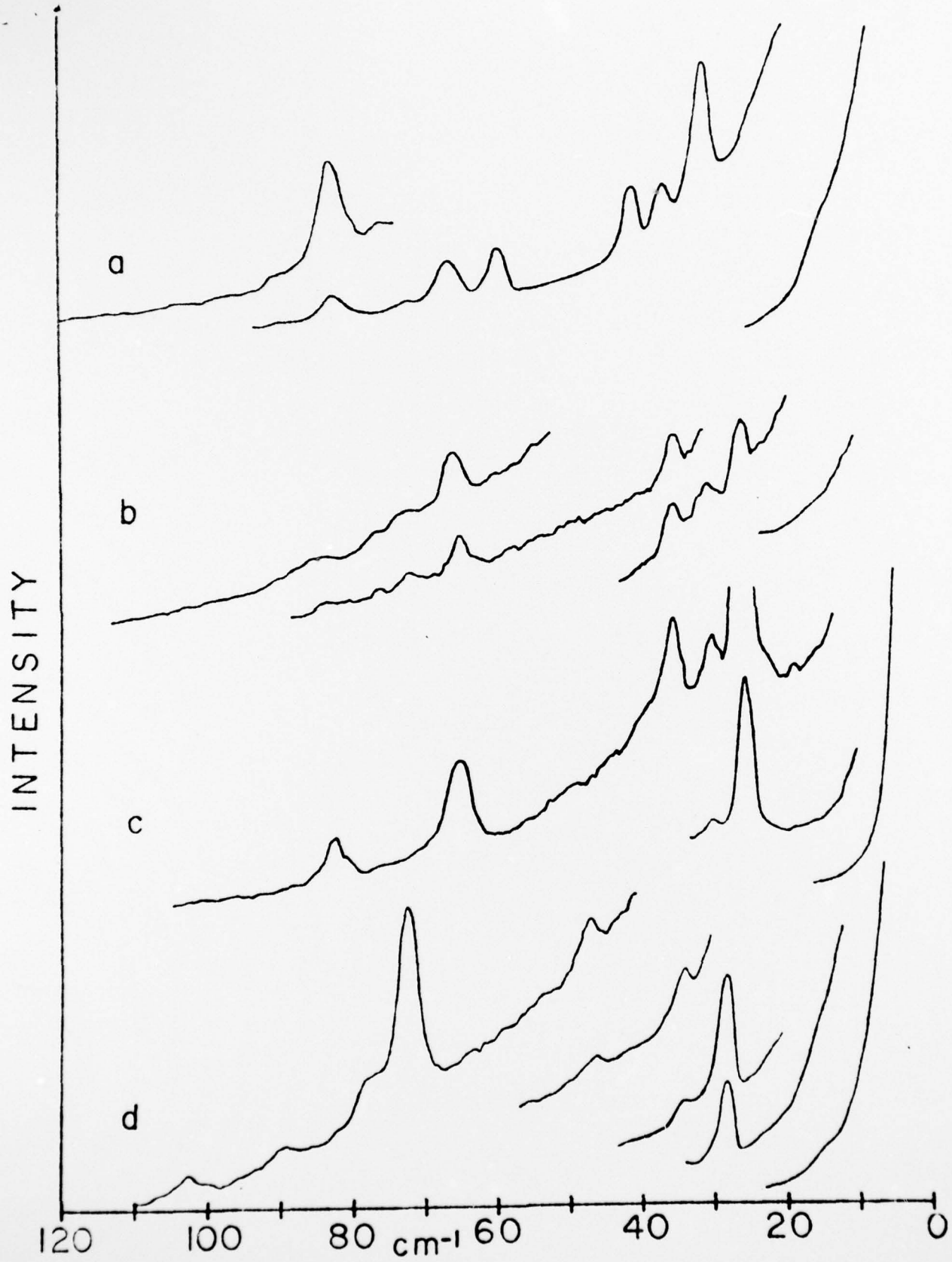
a
b
c
d
INTENSITY
120
100
80
cm-1
60
40
20
0

Figure 9. Evaluation of the idealized pure translational and pure rotational phonon model discussed in text. Plotted are the experimental frequencies ν_i (X = UF_6; □ = ReF_6; ∧ = WF_6; O = MoF_6). The dashed lines are plots of eq(1) (Section VC) for given arbitrary values of the slope. Values for M and I are given in Table 5. Lines which describe a given phonon mode are required to pass through the origin and several data points. A refers to purely translational motion and B refers to purely rotational motion. The assignments are summarized in Table 6.

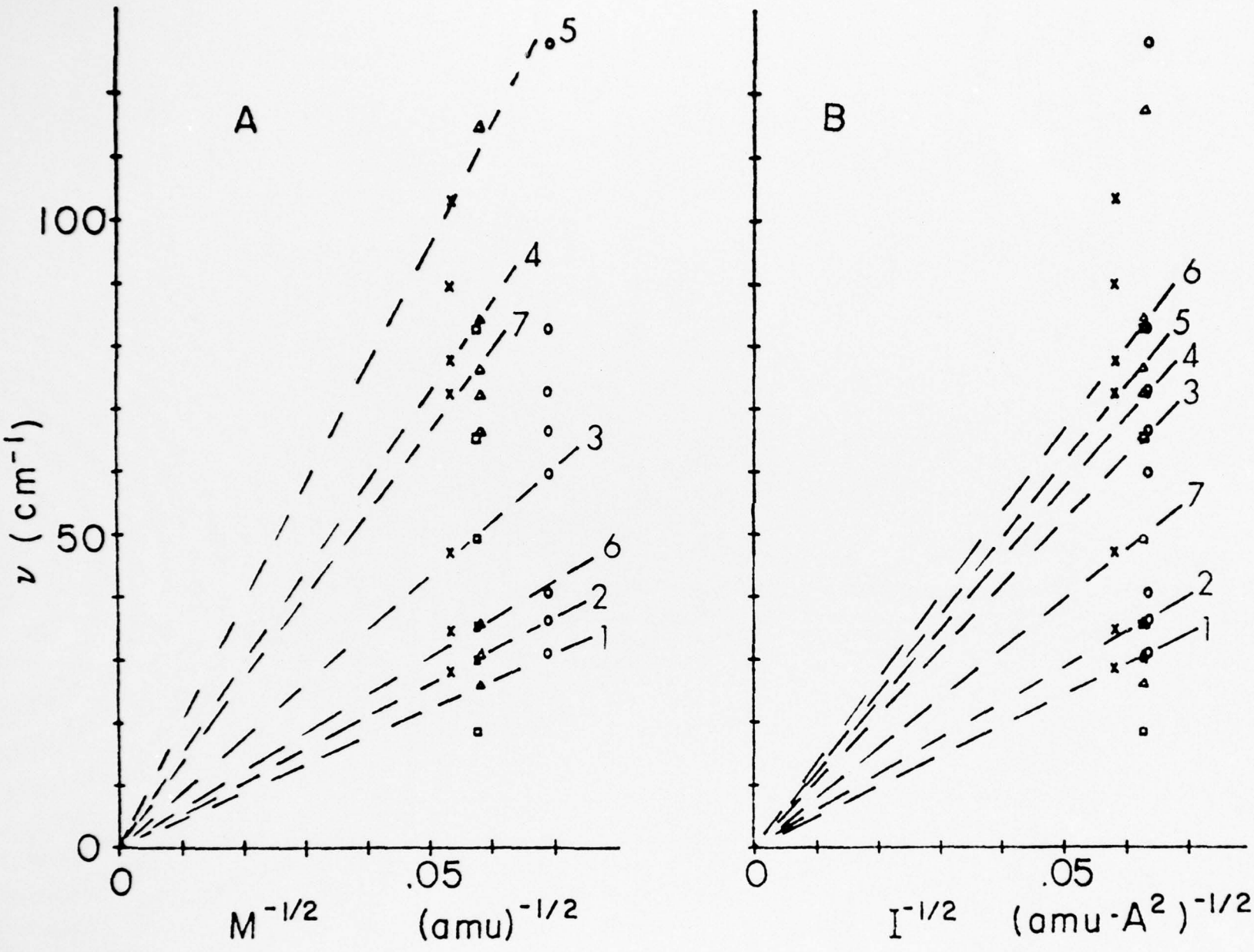
A
B
100
50
0
ν (cm⁻¹)
0
.05
M^-1/2 (amu)^-1/2
I^-1/2 (amu·A²)^-1/2
1
2
3
4
5
6
7

TECHNICAL REPORT DISTRIBUTION LIST

	No. Copies
Office of Naval Research Arlington, Virginia 22217 Attn: Code 472	2
Office of Naval Research Arlington, Virginia 22217 Attn: Code 102IP	6
ONR Branch Office 536 S. Clark Street Chicago, Illinois 60605 Attn: Dr. George Sandoz	1
ONR Branch Office 715 Broadway New York, New York 10003 Attn: Scientific Dept.	1
ONR Branch Office 1030 East Green Street Pasadena, California 91106 Attn: Dr. R. J. Marcus	1
ONR Branch Office 760 Market Street, Rm. 447 San Francisco, California 94102 Attn: Dr. P. A. Miller	1
ONR Branch Office 495 Summer Street Boston, Massachusetts 02210 Attn: Dr. L. H. Peebles	1
Director, Naval Research Laboratory Washington, D.C. 20390 Attn: Library, Code 2029 (ONRL) Technical Info. Div. Code 6100, 6170	6 1 1
The Asst. Secretary of the Navy (R&D) Department of the Navy Room 4E736, Pentagon Washington, D.C. 20350	1
Commander, Naval Air Systems Command Department of the Navy Washington, D.C. 20360 Attn: Code 310C (H. Rosenwasser)	1

	No. Copie
Defense Documentation Center Building 5, Cameron Station Alexandria, Virginia 22314	12
U.S. Army Research Office P.O. Box 12211 Research Triangle Park, North Carolina 27709 Attn: CRD-AA-IP	
Commander Naval Undersea Research & Development Center San Diego, California 92132 Attn: Technical Library, Code 133	1
Naval Weapons Center China Lake, California 93555 Attn: Head, Chemistry Division	1
Naval Civil Engineering Laboratory Port Hueneme, California 93041 Attn: Mr. W. S. Haynes	1
Professor O. Heinz Department of Physics & Chemistry Naval Postgraduate School Monterey, California 93940	
Dr. A. L. Slafkosky Scientific Advisor Commandant of the Marine Corps (Code RD-1) Washington, D.C. 20380	1

TECHNICAL REPORT DISTRIBUTION LIST

	No. Copies
Dr. M. A. El-Sayed University of California Department of Chemistry Los Angeles, California 90024	1
Dr. M. W. Windsor Washington State University Department of Chemistry Pullman, Washington 99163	
~~Dr. E. R. Bernstein~~ ~~Colorado State University~~ ~~Department of Chemistry~~ ~~Fort Collins, Colorado 80521~~	
Dr. C. A. Heller Naval Weapons Center Code 6059 China Lake, California 93555	1
Dr. G. Jones, II Boston University Department of Chemistry Boston, Massachusetts 02215	
Dr. M. H. Chisholm Chemistry Department Princeton, New Jersey 08540	1
Dr. J. R. MacDonald Code 6110 Chemistry Division Naval Research Laboratory Washington, D.C. 20375	1
Dr. G. B. Schuster Chemistry Department University of Illinois Urbana, Illinois 61801	1
Dr. E. M. Eyring University of Utah Department of Chemistry Salt Lake City, Utah	1
Dr. A. Adamson University of Southern California Department of Chemistry Los Angeles, California 90007	1
Dr. M. S. Wrighton Massachusetts Institute of Technology Department of Chemistry Cambridge, Massachusetts 02139	1